Proceedings of the International Association for Shell and Spatial Structures (IASS) Symposium 2009, Valencia
Evolution and Trends in Design, Analysis and Construction of Shell and Spatial Structures
28 September – 2 October 2009, Universidad Politecnica de Valencia, Spain
Alberto DOMINGO and Carlos LAZARO (eds.)

Morphing Multistable Textured Shells

Mohammad R. GOLABCHI*, Simon D. GUEST

*Department of Engineering, University of Cambridge
Trumpington Street, Cambridge CB2 1PZ, UK
mrg47@cam.ac.uk

Abstract

Forming surface features in a shell, and combining this 'texture' with prestress, can lead to a range of distinctive *multistable* properties. This paper is concerned with describing the structural properties of shell surfaces where local indentation and corrugation are used to replace the isotropic behaviour of the shell, and studies the possibilities of using these shells as morphing and multistable structures. By taking advantage of the anisotropic properties of the textured shell structure and further prestressing the shell, a range of interesting multistable properties can be achieved. This study investigates the properties of a particular example of a textured shell surface using experimental and computational techniques. Remarkably, these results shown that dimpled textured shells can achieve an effective Poisson's ratio in bending of close to -1, providing interesting insights into the remarkable multistable properties that textured shell surfaces can achieve.

Keywords: Multistable structures, Textured shells, Finite element simulation

1. Introduction

Local indentation and corrugation, or 'texture', in a shell surface can lead to distinctive structural behaviour. This study describes the investigation of the properties of a particular class of novel textured shell surface, where dimples are placed in the surface at regular intervals.

Ultimately, the aim of the current work is to use these shell structures as components of multistable morphing structures; such structures are designed to remain in one stable configuration until forced to move to another stable configuration. Multistable morphing structures have many applications. One application might be as a deployable structure, where the structure can transform from a stable compact configuration to an alternative extended configuration. Another application might be for use in reconfigurable aircraft, where geometry change leads to increased aerodynamic performance. An advantage of multistability is that energy is not required to maintain a structure within one stable configuration, but is only required to transform the structure between configurations.

Thin cylindrically curved shell structures can show multistable behaviour; and Section 2 will show the use of dimpled shells as bistable cylindrically curved shells. Note, however, that not all cylindrical shells are bistable; in particular, if they are made unstressed from isotropic materials, they are only stable in the initial configuration. Previously, bistability has been engendered in cylindrical shells by either using a non-isotropic material (Guest and Pellegrino [2]), or by imposing prestress on an isotropic shell (Kebadze *et al.* [3]). This study introduces the idea of forming surface features in the shell and combining it with prestressing in order to obtain a wide range of possible morphing and multistable behaviour; the structures that will be described in Section 2.2 combine prestressing and effective anisotropy. In order to understand this behaviour, we require knowledge of how a dimpled surface acts in an anisotropic manner, and this will be the main focus of the paper in Sections 3 and 4.

2. Bistable textured shells

This section demonstrates different techniques that can be used to create bistable structures from a doubly corrugated shell, and these will illustrate some initial ideas on the range of bistable properties that can be engendered.

Textured shells have small surface features at a scale intermediate between the overall structural scale, and the thickness of the shell (Norman *et al*. [4]). In this study we will consider a doubly corrugated shell, as shown in Figure 1. The experimental studies were conducted with a hardened Copper Beryllium shell formed by a punching process, whose shape we approximate for numerical studies by a doubly-sinusoidal surface described by:

$$z = \frac{d}{2}.sin\left(\frac{2\pi}{\lambda}x\right).sin\left(\frac{2\pi}{\lambda}y\right), \tag{1}$$

where d is the depth, and λ is the wavelength of the corrugations.

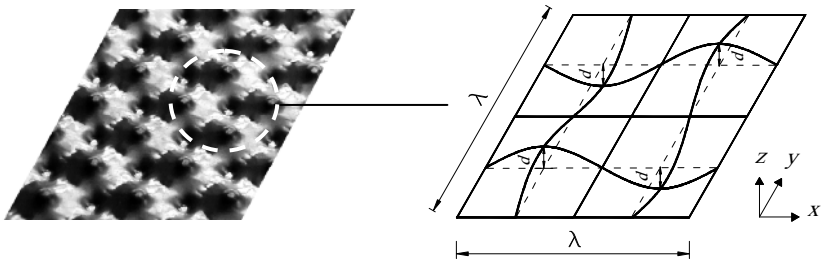

Figure 1: (a) The Copper-Beryllium shell used for experiments; (b) the assumed doubly-sinusoidal shell geometry used in the computational study.

The surface features in the structure ensure that the global properties of the shell are no longer isotropic; the dimpled surface has preferential directions for bending. The arrangement of dimples for this textured shell is depicted in Figure 2. It has been shown previously by Seffen [6, 7] that these dimpled sheets tend to bend about directions normal

to the least-packing of dimples; the shell has minimum bending stiffness about these directions.

In this study, the axis normal to the direction of least-packing of dimples is known as the "flexible axis", whereas, the axis normal to the direction with most-packing of dimples is known as the "stiff axis", and these directions are illustrated in Figure 2.

The dimpled sheets described above are globally flat; however, they can be formed into a globally cylindrical shape by plastically deforming the flat shell using a roller. In the following sections, we describe the range of behaviour that is engendered by this plastic forming process.

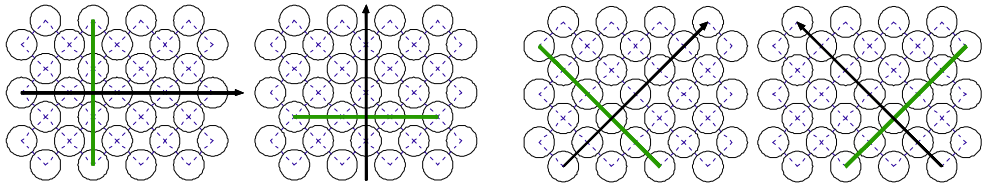

Figure 2: A representation of the dimpled surface, where each dimple (which are alternately up and down) is simply shown as a single circle. The dimples are arranged on a square grid. (a) The directions of least-packing between dimple centres define the flexible axes of the shell. (b) The directions of most-packing between dimple centres define the stiff axes of the shell.

2.1. Monostable Textured Shells

We find by experimentation that, if a flat dimpled sheet is rolled beyond its elastic limit in only one direction, either about its flexible or stiff axes, then it will form a cylindrical structure that is a monostable structure; it has only one stable equilibrium configuration. Thus, if the shell is elastically flattened, it will return to its original cylindrical configuration on release.

2.2. Bistable Textured Shells

Different behaviour can be observed if the shell is rolled consecutively in orthogonal directions. Two alternative schemes of orthogonal rolling can be followed; either the second rolling is in the *same sense* as the first, i.e., the centre of curvature lies on the same side of the shell surface, or the second rolling can be with *opposite-sense* bending.

2.2.1 Anticlastic bistable behaviour

If the initially flat corrugated shell is rolled beyond its elastic limit about a flexible axis, and is subsequently rolled in opposite-sense bending about the perpendicular flexible axis, again beyond the elastic limit, then the shell will finally behave as a bistable structure. The two stable states are shown in Figure 3. Note that the shell shows anticlastic bistable behaviour; the two stable states are curved in opposite senses. Plastic deformation of the surface has built up residual stresses in the shell that stabilise a second equilibrium state, in a similar manner to that described by Kebadze *et al.* [3] for a flat, isotropic shell.

Although the structure was formed by plastic deformation, switching between the two stable states appears to now be entirely repeatable, and is hence a purely elastic deformation.

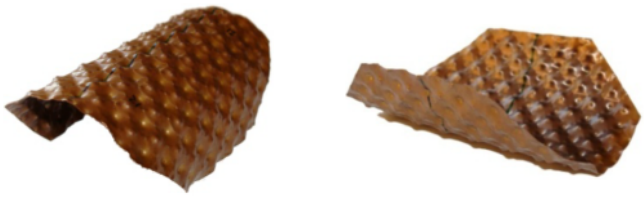

Figure 3: A doubly corrugated shell, showing *anticlastic* bistable behaviour.

2.2.2 Synclastic bistable behaviour

If the initially flat corrugated shell is rolled plastically about the two orthogonal flexible axes, but the second rolling is now in the *same* sense as the first, then we again generate a bistable structure, as shown in Figure 4. However, now the shell shows *synclastic* bistable behaviour – the two stable states are curved in the same sense. Again, switching between these two stable states is an elastic process. Note that this form of synclastic bistable behaviour is not possible for a flat isotropic sheet, even after prestressing.

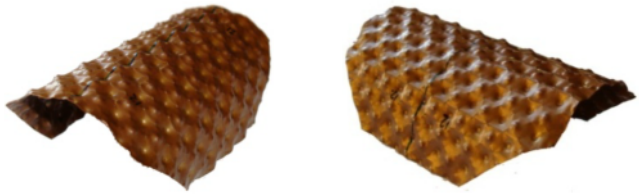

Figure 4: A doubly corrugated shell showing *synclastic* bistable behaviour.

2.2.3 Twisting behaviour

A third form of bistable behaviour can be engendered by plastically rolling the dimpled shell in the same sense about the two orthogonal *stiff* axes, to give the twisted synclastic bistable states shown in Figure 5. Note that the cylindrical axes in each case are now not perpendicular, and are not in the directions about which the shells were rolled. Again, this sort of behaviour would not be observed for a flat isotropic sheet.

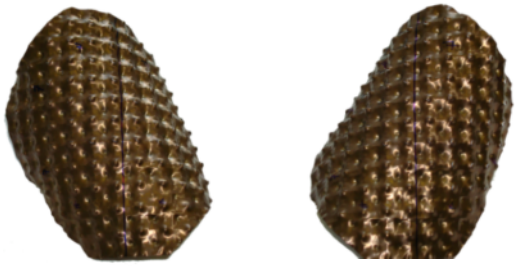

Figure 5: A doubly corrugated shell showing two twisted synclastic stable states.

2.3. Discussion

This section has shown three different ways in which the doubly-corrugated surface can form a bistable structure; in each case, the residual stresses left by plastic rolling processes was essential to the bistability. However, only the first, anticlastic, bistable response, shown in Figure 3, would be observed for a flat, undimpled isotropic sheet; the *texture* (dimples) of our shells was required to form the synclastic bistable states shown in Figures 4 and 5. The texture ensures that the shell has non-isotropic global behaviour, and the next sections will explore these non-isotropic properties.

3. Computational modeling of bending properties

This section investigates the effect of the *orientation* of corrugations on the bending behaviour of a doubly corrugated shell, and determines how the bending properties of the shell change by varying the direction of corrugations. The bending stiffness is determined by a computational simulation of a simple three-point bending test, as shown in Figure 6. To compute the effect of the orientation of corrugations, ϕ, on the bending stiffness of the doubly corrugated shell, we calculate the stiffness of the structure relative to the stiffness of an equivalent flat plate, K/K_{flat} for various angles ϕ. In each case, the ratio of the depth of corrugation to the thickness of the shell was $d/t = 2.37$ and the ratio of the wavelength to the depth of the corrugations was $\lambda/d = 5.56$, matching the physical shells shown in Section 2.

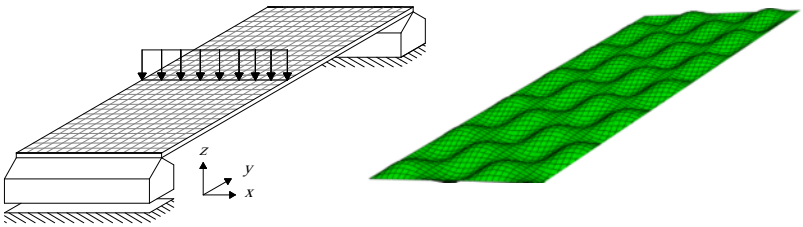

Figure 6: Sketch of the textured shell on its supports and the FE model for $\phi = 0°$. Note that the loading applied is displacement controlled; the shell is uniformly displaced along its centre-line.

To evaluate the effect of the orientation of corrugations, the corrugated surface will be defined by a rotated form of Equation (1),

$$z = \frac{d}{2}.sin\left(\frac{2\pi}{\lambda}(x\,cos\,\phi + y\,sin\,\phi)\right).sin\left(\frac{2\pi}{\lambda}(-x\,sin\,\phi + y\,cos\,\phi)\right) . \quad (2)$$

3.1. Results and discussions

In this section the results of the FE simulation of the doubly corrugated shell are presented. Firstly, the effect of corrugation orientation on the stiffness of a shell for a single width/length ratio is given. Secondly, the variations of this effect for different width/length ratios are described.

3.1.2. Results for a shell with a width/length ratio of 0.5

The shells described in this section all have a constant ratio of width/length equal to $W/L = 0.5$, and are modelled by a mesh of 50 by 100 elements. Figure 7 illustrates the variation of the bending stiffness of these shells with the corrugation angle, and also with the effect of the position of the origin of the coordinates defining the corrugation, described as the 'corrugation offset'.

There are a number of points to note about these results. Firstly, the results are symmetric about $\phi = 0°$ and $\phi = 45°$, as may be expected from the symmetry of the dimpled surface. Secondly, the stiffness is a minimum at $\phi = 0°$ and integer multiples of ϕ =90°; the reason for this is that, for these orientations, there are lines running across the shell where the corrugation gives no extra thickness, as shown in Figure 8, and these flexible regions dominate the structural behaviour. Thirdly, the stiffness is a maximum at around $\phi = 45°$; however, here the results become noisy. The stiffness around $\phi = 45°$ is highly sensitive to the exact location of the origin in equation (2) – we believe this is due to the detail of the relative position of the boundaries with respect to the corrugation.

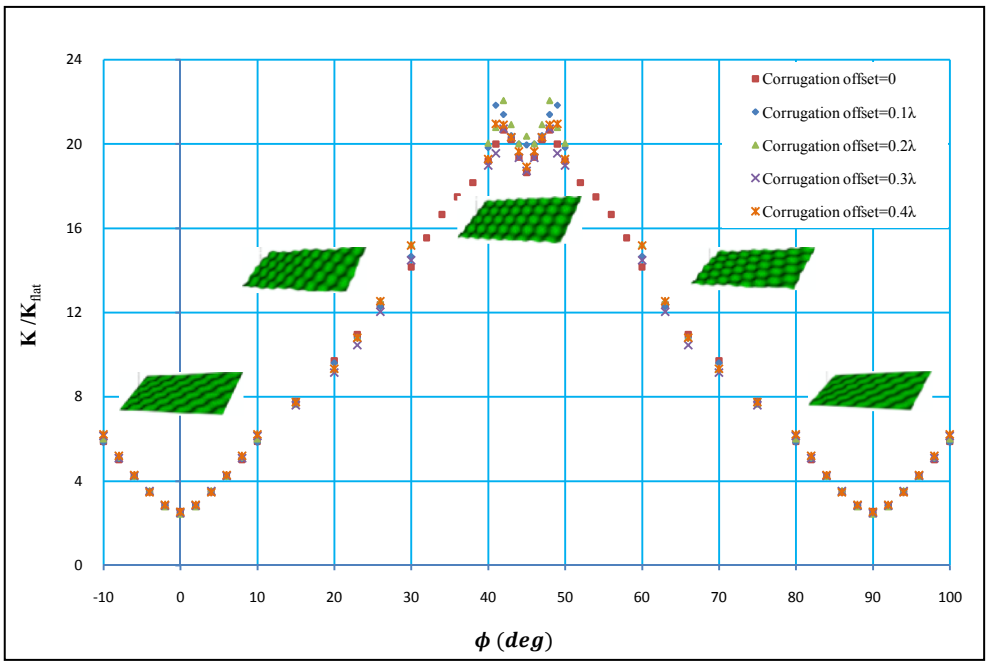

Figure 7: Variation of the bending stiffness with the orientation of corrugations. Results are presented for five different corrugation offsets, where in each case the relative position of the corrugations is shifted along the $x = y$ direction.

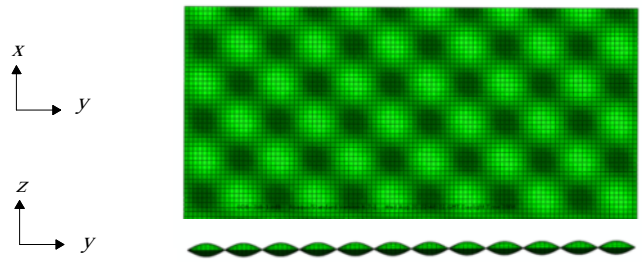

Figure 8: Top and side view of a doubly corrugated shell for $\phi = 0°$, showing lines running across the shell where the corrugation gives not additional thickness.

3.1.2. Results for shells with different ratios of width/length

In this section the variation of the bending stiffness of the shell with corrugation angle for different ratios of width/length are studied. For simplicity, we don't consider the effect of corrugation offset. The results are depicted in Figure 9.

The key point to note in Figure 9 is that, for a narrow shell, e.g. $W/L < 0.5$, there is little variation in the bending stiffness with the orientation of corrugation, whereas for a wide shell, e.g. $W/L > 2$, the variation in bending stiffness is very marked. This becomes more clear by considering the variation of the bending stiffness with W/L for bending about the flexible axis, $\phi = 0°$, and about the stiff axis, $\phi = 45°$. For $\phi = 0°$ the bending stiffness relative to that of a flat plate varies little with W/L, but for $\phi = 45°$ the bending stiffness relative to that of a flat plate varies greatly.

The reason for this increase in the relative bending stiffness of the wider shells is due to the coupling between bending in two directions, and this is clearly shown in the displaced shell configurations shown in Figure 10. It can be seen that in bending the corrugated shell about the flexible axis, $\phi = 0°$, there is almost no coupling between bending in the x and y directions. In this case the shell responds in *cylindrical bending*. The distance to the free edge of the shell little affects the bending response, and hence there is little variation in relative stiffness with W/L. By contrast for bending about the stiff axis, $\phi = 45°$, there is a strong coupling between bending in the x and y directions. Therefore, the textured shell will have a doubly curved surface and will respond in *spatial bending*; the distance to the free edge of the shell significantly affects the bending response, and hence there is large variation in relative stiffness with W/L.

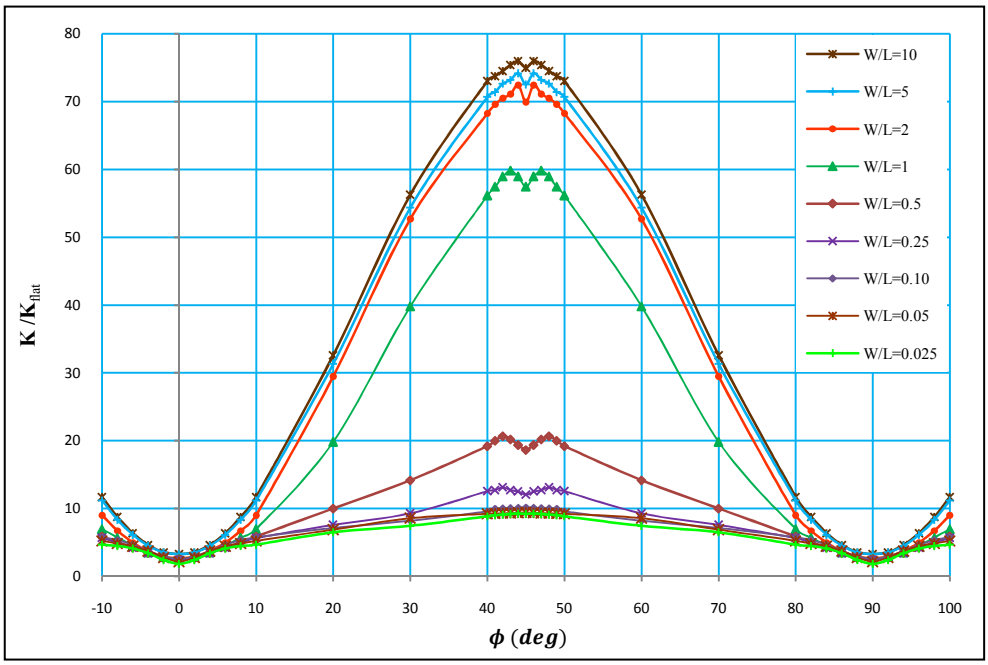

Figure 9: Variation of the relative bending stiffness with bending orientation for shells with different ratios of width/length.

4. Estimation of the bending coupling parameter

Comparing the results for a very narrow and very wide strip of the textured shell enables us to quantify the bending coupling in the shell and hence to predict the effective Poisson's ratio. This section describes a simplified analytical calculation to find relationships between the components of the bending stiffness matrix. This calculation is important in considering bistability, as Guest and Pellegrino [2] have shown that bistability in cylindrical curved shells is dependent on the relative magnitudes of the component of the bending stiffness matrix; increasing the coupling between bending in two directions will tend to create bistability in the structure.

4.1. Analytical calculation

From the generalized Hooke's law for an element of a shell a constitutive bending relationship is given by (Calladine [1]):

$$\mathbf{M} = \mathbf{D}.\boldsymbol{\kappa}\,, \tag{4}$$

$$\begin{bmatrix} M_x \\ M_y \\ M_{xy} \end{bmatrix} = \begin{bmatrix} D_{11} & D_{12} & D_{16} \\ D_{21} & D_{22} & D_{26} \\ D_{61} & D_{62} & D_{66} \end{bmatrix} \begin{bmatrix} \kappa_x \\ \kappa_y \\ \kappa_{xy} \end{bmatrix}. \tag{5}$$

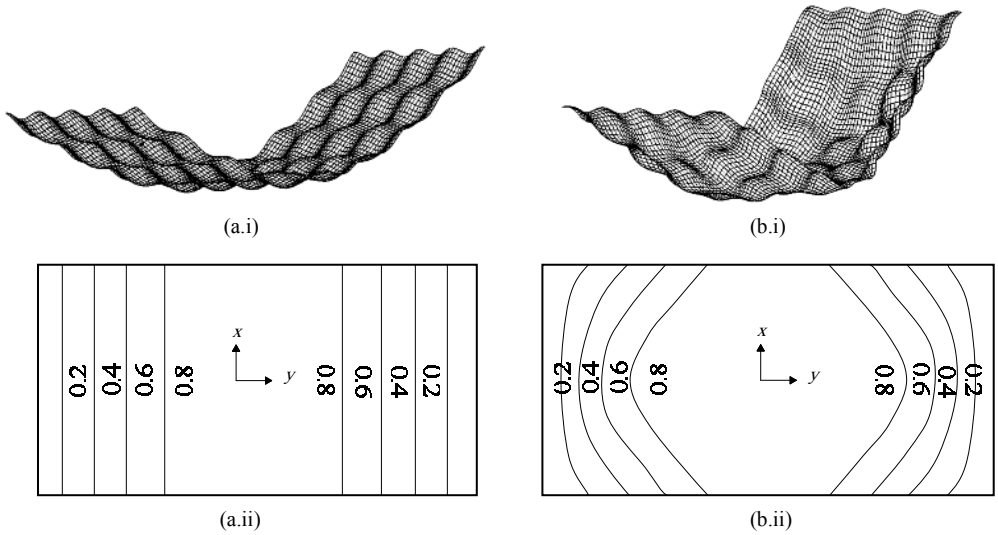

Figure 10: Bending behaviour of the textured shell for $W/L = 0.5$ for (a) $\phi = 0°$, and (b) $\phi = 45°$; for each case the deformed shape of the structure is shown in (i), and a contour plot of the relative magnitude of the vertical deformation is shown in (ii). (a) For the case $\phi = 0°$, there is little coupling between bending in the *x* and *y* directions, and we describe the bending as 'cylindrical' (b) For the case $\phi = 45°$, it is clear that there is coupling between bending in the the *x* and *y* directions (the shell takes up a bowl shape), and we describe the bending as 'spatial'.

In the present case, the structure is orthotropic for $\phi = 0°$ and $\phi = 45°$, and hence four of the terms of the bending stiffness matrix are zero, $D_{16} = D_{26} = D_{61} = D_{62} = 0$; for simplicity, we will extend this, and assume that there is no coupling between bending and twisting for all ϕ. Further, D_{21} and D_{12} are equal, and because orthogonal directions are equivalent, $D_{22} = D_{11}$. Thus the curvatures in the *x* and *y* directions are given by:

$$\begin{bmatrix}\kappa_x \\ \kappa_y\end{bmatrix} = \frac{1}{{D_{11}}^2 - {D_{12}}^2}\begin{bmatrix}D_{11} & -D_{12} \\ -D_{12} & D_{11}\end{bmatrix}\begin{bmatrix}M_x \\ M_y\end{bmatrix}. \tag{6}$$

For a narrow strip of the textured shell, we assume that there is no moment along the transverse direction of the shell ('equivalent' to plane stress). Therefore, we can write:

$$\begin{cases}M_x \neq 0 \\ M_y = 0\end{cases} \tag{7}$$

Substituting equation (7) into equation (6), we obtain the following equation for the curvature in *x* and *y* directions:

$$\kappa_x = \left(\frac{D_{11}}{{D_{11}}^2 - {D_{12}}^2} \right) M_x \ , \tag{8}$$

$$\kappa_y = -\frac{D_{12}}{D_{11}} \, k_x \ . \tag{9}$$

From equation (8) the bending stiffness α for a narrow strip of a corrugated shell in the x direction can be written as:

$$\frac{M_x}{\kappa_x} = D_{11} - \frac{{D_{12}}^2}{D_{11}} = \alpha \ . \tag{10}$$

Alternatively, for a wide strip of the textured shell, we assume there is no curvature along the transverse direction of the shell, ('equivalent' to plane strain). Therefore, we can write:

$$\begin{cases} \kappa_x \neq 0 \\ \kappa_y = 0 \end{cases} \tag{11}$$

Thus, by replacing equation (11) into equation (6), the following equation can be written for the bending moments in x and y directions:

$$M_x = D_{11} \, \kappa_x \ , \tag{12}$$

$$M_y = \frac{D_{12}}{D_{11}} \, M_x \ . \tag{13}$$

From equation (12), the bending stiffness β of a wide strip of the shell is given by:

$$\frac{M_x}{\kappa_x} = D_{11} = \beta \ . \tag{14}$$

We can estimate the relative values of the bending stiffness of a narrow strip α to the bending stiffness of a wide strip β from the FE simulations, and thus we can estimate, from equations (13) and (14) that the coupling between bending in two directions is given by

$$\frac{D_{12}}{D_{11}} = \pm \sqrt{1 - \frac{\alpha}{\beta}} \ . \tag{15}$$

The ratio D_{12}/D_{11} is the negative of the effective Poisson's ratio. We cannot from this analysis calculate whether D_{12} is positive or negative; however, the distinctive 'bowl' shape seen in Figure 10 shows synclastic bending, a negative effective Poisson's ratio, and hence a positive value of the ratio D_{12}/D_{11}.

4.2. Results for the bending coupling

In order to estimate the bending coupling parameter of the shell, we assume the values obtained previously for the bending stiffness of the longest and widest shell presented in Figure 9 as the bending stiffness for a narrow and wide strip. Now by substituting these values in equation (15), and assuming a negative effective Poisson's ratio, we can obtain a new graph that illustrates the variation of the bending coupling term with corrugation angle.

Figure 11 depicts the variation of $\nu = -D_{12}/D_{11}$ with orientation of corrugation. It can be seen that for bending about the flexible axis, $\phi = 0°$, the coupling between bending in two orthogonal directions is negligible. However, as the corrugation angle increases, the coupling between bending in two directions increases rapidly and the shell tends to have a bowl shape deformation. Remarkably, the effective Poisson's ratio for this textured shell in bending about the stiff axis is very close to -1, showing the strong coupling between bending in the *x* and *y* directions.

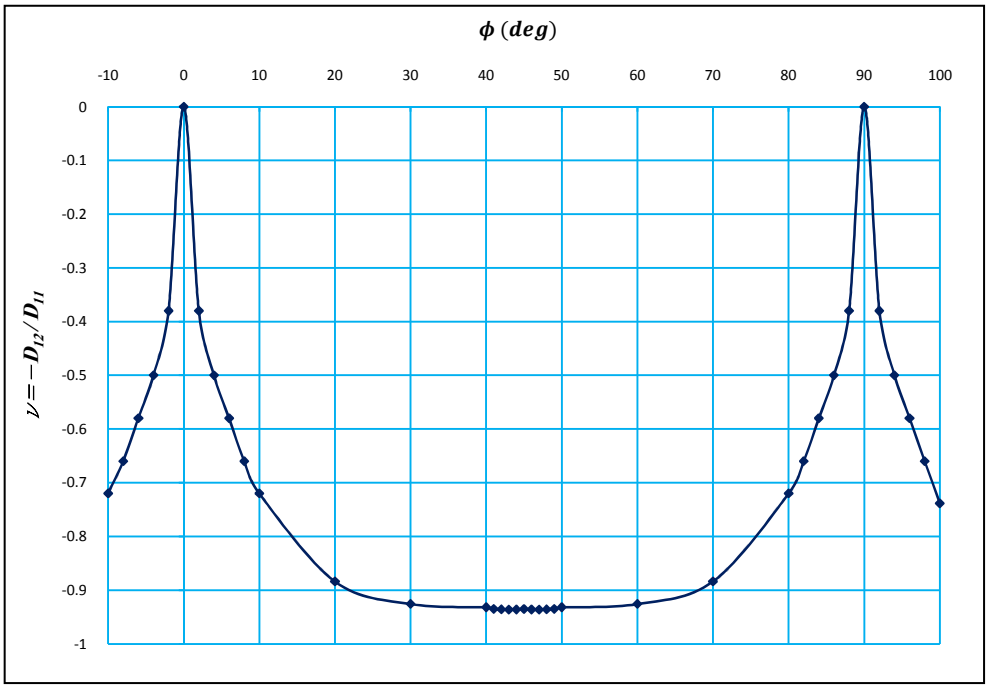

Figure 11: Variation of effective Poisson's ratio $\nu = -D_{12}/D_{11}$ with orientation of corrugation.

5. Conclusions

The computational results in this paper have shown that dimpled 'textured' shells can achieve an effective Poisson's ratio in bending of close to -1. This remarkable Poisson's ratio shows a strong coupling between bending in orthogonal directions and illustrates the possibility of using these textured shells as multistable structures. It is interesting to note the close correlation of this result with those shown by Schenk and Guest [5] for a related faceted surface.

The results presented in this study provide interesting insights for explaining the effective multistable properties of the textured shell surfaces that allow such structures to exist. Further work is being undertaken to measure the bending properties of the dimpled shells experimentally, and also to determine the effect of the twisting stiffness on the overall behaviour of the textured shell structure.

References

[1] Calladine C. R., (1983), *Theory of Shell Structures*. Cambridge University Press, Cambridge.

[2] Guest S.D. and Pellegrino S., (2006), "Analytical models for bistable cylindrical shells". *Proceedings of the Royal Society: Mathematical, Physical & Engineering Sciences*. 462(2067), 839-854.

[3] Kebadze E., Guest S.D. and Pellegrino S., (2004), "Bistable prestressed shell structures". *International Journal of Solids and Structures*. 41(11-12), 2801-2820.

[4] Norman A.D., Golabchi M.R., Seffen K.A. and Guest S.D., (2008), "Multistable Textured Shell Structures". *Advances in Science and Technology*, 54, 168-173, presented at CIMTEC 2008, Acireale, Sicily, Italy, 8-13 June, 2008.

[5] Schenk M. and Guest S.D., (2009), "Folded Textured Sheets". *IASS 2009. Evolution and Trends in Design, Analysis and Construction of Shell and Spatial Structures*, Valencia, Spain, 28 Sep-2 Oct, 2009.

[6] Seffen K. A., (2007), "Hierarchical Multi-stable Shapes in Mechanical Memory Metal". *Scripta Materilia*, 56(5), pp.417-420.

[7] Seffen K. A., (2006), "Mechanical Memory Metal: a Novel Material for Developing Morphing Engineering Structures". *Scripta Materilia*, 55(4), pp.411-414.